



## Modelling Mechanical Properties of Self-Compacting Rice Husk Ash Concrete Using Artificial Neural Network

Emmanuel E. NDUBUBA<sup>1</sup>, Joseph O. ENOCK<sup>2\*</sup>, Innocent T. NTEYOHO<sup>3</sup>

<sup>1,2,3</sup>Department of Civil Engineering, University of Abuja, Abuja, Nigeria

<sup>1</sup>[emanuel.ndububa@uniabuja.edu.ng](mailto:emanuel.ndububa@uniabuja.edu.ng), <sup>2\*</sup>[engrenockjoseph@gmail.com](mailto:engrenockjoseph@gmail.com), <sup>3</sup>[nteyohoinnocent@gmail.com](mailto:nteyohoinnocent@gmail.com)

### Abstract

This study investigates the effects of Rice Husk Ash (RHA) on the mechanical properties and workability of Self-Compacting Concrete (SCC), focusing on compressive and flexural strengths. The mixes incorporated Hydroplast 260GR, a high-range water-reducing admixture (super-plasticizer), at dosages of up to 2.0% of the cement weight to achieve the high flowability required for self-compacting concrete (SCC) while minimizing overall water demand. Using a dataset of 56 concrete mix proportions developed using simplex lattice design method (N[6,3]) to systematically access the effect of varying Rice Husk Ash (RHA) content on the investigated performance parameters which include compressive strength, flexural strength and workability. The experimental analysis revealed a decline in compressive strength from 20 MPa to 11 MPa and flexural strength from 3.0 MPa to 2.2 MPa as RHA increased, though low RHA levels (5%–10%) occasionally matched the control due to pozzolanic effects. Workability remained stable (slump values 550–650 mm) up to 20% RHA, indicating minimal impact on flowability. Predictive models, including Linear Regression (LR) and Artificial Neural Network (ANN), were developed to estimate mechanical properties, with the dataset split into 80% training and 20% testing. The LR model outperformed the ANN, achieving RMSE values of 0.103 for flexural strength and 1.240 for compressive strength, compared to the ANN's 0.374 ( $R^2 = 0.89$ ) and 2.074 ( $R^2 = 0.09$ ), respectively, highlighting the LR's suitability for RHA-SCC predictions given the dataset's linear tendencies and size constraints. Correlation analysis showed strong relationships between cement, water, and RHA, with RHA negatively affecting strength ( $r \approx -0.48$  to  $-0.51$ ). The study recommends limiting RHA to 5–10% for practical applications, refining the ANN with a larger dataset, and exploring non-linear models to improve compressive strength predictions, providing a foundation for sustainable SCC design.

**Keywords:** Rice Husk Ash, Artificial Neural Network, Linear Regression, Self-compacting concrete, super-plasticizer.

### 1.0 Introduction

Concrete has long been a primary construction material. However, current construction demands for durability and performance, along with solutions to challenges such as improper vibration in congested reinforcements has driven interest in self-compacting concrete (SCC), which flows without vibration. SCC was developed in Japan in the late 1980s to address the need for highly workable concrete that can fill formwork and pass through dense reinforcement without compaction [1]. Its benefits include improved surface finishes, reduced labor and noise, and faster construction. SCC must exhibit filling ability, passing ability, and segregation resistance. Achieving this balance requires careful mix design, which remains more complex than for vibrated concrete (VC). Though many mix design approaches exist [2], no single global method has been universally adopted. Super-plasticizers are commonly used in SCC to enhance flowability while maintaining strength. [3] Observed that they reduce water content and improve mechanical integrity. Segregation can be controlled by adding powder or viscosity modifiers, often using industrial by-products like limestone powder, fly ash, or slag [4], [5], which also reduce environmental impact and cost [6]. Portland cement accounts for over 5% of global CO<sub>2</sub> emissions [6]. Green materials like fly ash and groundnut shell ash have been used to partially replace cement. Rice Husk Ash (RHA), derived from burning rice husks under controlled conditions (<800°C), is rich in amorphous silica and alumina, making it highly pozzolanic. Despite its proven benefits in conventional concrete, RHA has seen limited use in SCC. RHA, produced during rice milling and combustion, contains 85–90% amorphous silica [7] [8]. Its pozzolanic activity improves strength by refining pore structure and reducing porosity. Improper disposal of RHA poses environmental risks. Studies on SCC incorporating 10% and 20% RHA showed increased compressive strength at 56 days due to RHA's filler and pozzolanic effects. Combined with additives like fly ash or limestone powder, RHA further enhances packing density and strength. In civil engineering, artificial intelligence, especially Artificial Neural Networks (ANN), has gained traction. ANN mimics human cognition through interconnected processing units (neurons) and was first proposed by McCulloch and Pitts in 1943 [9]. Modern ANN models such as SOM, RBF, MLP, and Neuro-Fuzzy use algorithms like backpropagation and reinforcement learning for tasks like estimation, pattern recognition, and forecasting [10]. ANN began to be applied in civil engineering in the

late 1980s, especially for predicting concrete properties. For instance, Mulusew used ANN and fuzzy logic to assess the effects of slag on concrete strength [11]. ANN has outperformed traditional regression in modeling high-performance concrete properties such as compressive strength and permeability [12], and has also been used for lightweight concrete prediction. ANNs learn from input-output data and generalize to handle non-linear relationships. They typically comprise input, hidden, and output layers, and operate through topology (network structure), learning (data storage), and recall (information retrieval). Compared to traditional statistical models, which require known relationships among variables, ANN can adaptively learn both linear and non-linear patterns [13]. Techniques like ANN, fuzzy logic, and ANFIS are often simpler and more accurate than mathematical models. ANN has been used to predict compressive strength, modulus of elasticity, structural performance, and even in non-destructive testing [14],[15],[16],[17],[18],[19],[20],[21]. This study therefore, aims to apply the use of artificial neural network as a tool to provide a more accurate estimation for the modelling of the mechanical properties of Rice Husk Ash Concrete. The appropriate mix design for the evaluation of self-compacting incorporated with Rice Husk concrete at varying percentage replacements of cement with Rice Husk Ash is established, evaluation of the flexural and compressive strength of the resulting mixture is tested. And the neural network model is developed and use to make predictions of the compressive and flexural strengths of the established SCC mix.

## 2.0 Materials and Methods

Ordinary Portland cement of grade 42.5 was adopted for this study, the fine and coarse aggregate used were sourced locally. Rice husk was sourced from Lambata in Kwali area council, the properties of super-plasticizer, Hydroplast 260GR used, is shown in Table 1, obtained from the manufacturer.

Table 1: Properties of Hydroplast 260GR

SN		
1	Colour	Brown
2	Density	1.16g/cm <sup>3</sup>
3	Chloride content	"Chloride-free" to EN 934
4	Freezing point	0°C
5	PH	7-9

Physical properties examination of the aggregates was done to ascertain the suitability of the aggregate for the mixture: The aggregate test results fall within acceptable limits specified by ASTM International and British Standards Institution. The materials exhibited a specific gravity of 2.65 and bulk density of 1550 kg/m<sup>3</sup>, indicating normal-weight aggregates with adequate strength. The moisture content (1.2%) was low and unlikely to significantly affect the mix water demand. The grading was well-distributed, with a fineness modulus of 2.6 for the fine aggregate, supporting good workability and reduced voids. Mechanical properties were also satisfactory, with an aggregate crushing value of 24% and a Los Angeles abrasion value of 28%, both within recommended limits for structural concrete. Overall, the aggregates demonstrate suitable strength, durability, and grading characteristics for use in the concrete mixture. Using the simplex lattice technique and adopting the third-degree polynomial approach for six components, a mix formulation was obtained for the experiment as shown in Table 2 and Table 3. Three cubes of 150 mm x 150 mm were casted for each mix point. The cured cube was then subjected to a compressive strength test. The same was done to obtain the flexural strength using the 100 mm x 100 mm x 400 mould. The evaluation of predictive models for the flexural and compressive strengths of Self-Compacting Concrete (SCC) was carried out to obtain a comprehensive comparison between a linear regression model and an artificial neural network (ANN) model, utilizing a dataset of 56 samples split into 80% training (approximately 45 samples) and 20% testing (approximately 11 samples). The ANN model contained two dense hidden layers of 60 and 32 and a dropout layer was applied at 20%, the activation function adopted was the 'relu' and the optimizer was 'Adam', a learning rate of 0.001 was applied, and an early stop was applied at a patience level of 10, the batch size of 16 was used with 250 epochs. The architect of the ANN used is shown in Figure 1.

Table 2: Matrix table for simplex lattice formulation

		PSEUDO COMPONENT						REAL COMPONENTS					
S/No.	MIXTURE POINTS	X1	X2	X3	X4	X5	X6	Z1	Z2	Z3	Z4	Z5	Z6
								Water	Cement	RHA	Fine Agg	Super Plast.	coarse agg
1	R1	1	0	0	0	0	0	0.700	1.000	0.000	2.200	0.015	2.000
2	R2	0	1	0	0	0	0	0.700	0.950	0.050	2.200	0.016	2.000
3	R3	0	0	1	0	0	0	0.700	0.900	0.100	2.200	0.017	2.000
4	R4	0	0	0	1	0	0	0.700	0.850	0.150	2.200	0.018	2.000
5	R5	0	0	0	0	1	0	0.700	0.800	0.200	2.200	0.019	2.000
6	R6	0	0	0	0	0	1	0.700	0.750	0.250	2.200	0.020	2.000
7	R12	0.5	0.5	0	0	0	0	0.700	0.975	0.025	2.200	0.016	2.000
8	R13	0.5	0	0.5	0	0	0	0.700	0.950	0.050	2.200	0.016	2.000
9	R14	0.5	0	0	0.5	0	0	0.700	0.925	0.075	2.200	0.017	2.000
10	R15	0.5	0	0	0	0.5	0	0.700	0.900	0.100	2.200	0.017	2.000
11	R16	0.5	0	0	0	0	0.5	0.700	0.875	0.125	2.200	0.018	2.000
12	R23	0	0.5	0.5	0	0	0	0.700	0.925	0.075	2.200	0.017	2.000
13	R24	0	0.5	0	0.5	0	0	0.7	0.900	0.100	2.200	0.017	2.000
14	R25	0	0.5	0	0	0.5	0	0.700	0.875	0.125	2.200	0.018	2.000
15	R26	0	0.5	0	0	0	0.5	0.700	0.850	0.150	2.200	0.018	2.000
16	R34	0	0	0.5	0.5	0	0	0.700	0.875	0.125	2.200	0.018	2.000
17	R35	0	0	0.5	0	0.5	0	0.700	0.850	0.150	2.200	0.018	2.000
18	R36	0	0	0.5	0	0	0.5	0.700	0.825	0.175	2.200	0.019	2.000
19	R45	0	0	0	0.5	0.5	0	0.700	0.825	0.175	2.200	0.019	2.000
20	R46	0	0	0	0.5	0	0.5	0.700	0.800	0.200	2.200	0.019	2.000
21	R56	0	0	0	0	0.5	0.5	0.700	0.775	0.225	2.200	0.020	2.000

22	R123	0.33	0.33	0.33	0	0	0	0.693	0.941	0.050	2.178	0.016	1.980
23	R124	0.33	0.33	0	0.33	0	0	0.693	0.924	0.066	2.178	0.016	1.980
24	R125	0.33	0.33	0	0	0.33	0	0.693	0.908	0.083	2.178	0.017	1.980
25	R126	0.33	0.33	0	0	0	0.33	0.693	0.891	0.099	2.178	0.017	1.980
26	R134	0.33	0	0.33	0.33	0	0	0.693	0.908	0.083	2.178	0.017	1.980
27	R135	0.33	0	0.33	0	0.33	0	0.693	0.891	0.099	2.178	0.017	1.980
28	R136	0.33	0	0.33	0	0	0.33	0.693	0.875	0.116	2.178	0.017	1.980
29	R145	0.33	0	0	0.33	0.33	0	0.693	0.875	0.116	2.178	0.017	1.980
30	R146	0.33	0	0	0.33	0	0.33	0.693	0.858	0.132	2.178	0.017	1.980
31	R156	0.33	0	0	0	0.33	0.33	0.693	0.842	0.149	2.178	0.018	1.980
32	R234	0	0.33	0.33	0.33	0	0	0.693	0.891	0.099	2.178	0.017	1.980
33	R235	0	0.33	0.33	0	0.33	0	0.693	0.875	0.116	2.178	0.017	1.980
34	R236	0	0.33	0.33	0	0	0.33	0.693	0.858	0.132	2.178	0.017	1.980
35	R245	0	0.33	0	0.33	0.33	0	0.693	0.858	0.132	2.178	0.017	1.980
36	R246	0	0.33	0	0.33	0	0.33	0.693	0.842	0.149	2.178	0.018	1.980
37	R256	0	0.33	0	0	0.33	0.33	0.693	0.825	0.165	2.178	0.018	1.980
38	R112	0.66	0.33	0	0	0	0	0.693	0.974	0.017	2.178	0.015	1.980
39	R113	0.66	0	0.33	0	0	0	0.693	0.957	0.033	2.178	0.016	1.980
40	R114	0.66	0	0	0.33	0	0	0.693	0.941	0.050	2.178	0.016	1.980
41	R115	0.66	0	0	0	0.33	0	0.693	0.924	0.066	2.178	0.016	1.980
42	R116	0.66	0	0	0	0	0.33	0.693	0.908	0.083	2.178	0.017	1.980
43	R221	0.33	0.66	0	0	0	0	0.693	0.957	0.033	2.178	0.016	1.980
44	R223	0	0.66	0.33	0	0	0	0.693	0.924	0.066	2.178	0.016	1.980
45	R224	0	0.66	0	0.33	0	0	0.693	0.908	0.083	2.178	0.017	1.980
46	R225	0	0.66	0	0	0.33	0	0.693	0.891	0.099	2.178	0.017	1.980
47	R226	0	0.66	0	0	0	0.33	0.693	0.875	0.116	2.178	0.017	1.980
48	R331	0.33	0	0.66	0	0	0	0.693	0.924	0.066	2.178	0.016	1.980
49	R332	0	0.33	0.66	0	0	0	0.693	0.908	0.083	2.178	0.017	1.980

50	R334	0	0	0.66	0.33	0	0	0.693	0.875	0.116	2.178	0.017	1.980
51	R335	0	0	0.66	0	0.33	0	0.693	0.858	0.132	2.178	0.017	1.980
52	R336	0	0	0.66	0	0	0.33	0.693	0.842	0.149	2.178	0.018	1.980
53	R441	0.33	0	0	0.66	0	0	0.693	0.891	0.099	2.178	0.017	1.980
54	R442	0	0.33	0	0.66	0	0	0.693	0.875	0.116	2.178	0.017	1.980
55	R443	0	0	0.33	0.66	0	0	0.693	0.858	0.132	2.178	0.017	1.980
56	R445	0	0	0	0.66	0.33	0	0.693	0.825	0.165	2.178	0.018	1.980
57	R446	0	0	0	0.66	0	0.33	0.693	0.809	0.182	2.178	0.018	1.980
58	R551	0.33	0	0	0	0.66	0	0.693	0.858	0.132	2.178	0.017	1.980
59	R553	0	0	0.33	0	0.66	0	0.693	0.825	0.165	2.178	0.018	1.980
60	R556	0	0	0	0	0.66	0.33	0.693	0.776	0.215	2.178	0.019	1.980

Table 3: Mix proportions

	Water	Cement	RHA	Fine Agg.	Super Plast.	Coarse Agg.
Density (kg/cum) =	1000	1440	1350	1711	1160	2152
Samples	A1	A2	A3	A4	A5	A6
S1	0.652	0.932	0	2.436	0.014	2.785
S2	0.620	0.885	0.044	2.436	0.014	2.785
S3	0.587	0.838	0.087	2.435	0.014	2.784
S4	0.554	0.792	0.131	2.435	0.014	2.784
S5	0.522	0.745	0.175	2.434	0.014	2.783
S6	0.489	0.698	0.218	2.434	0.014	2.783
S7	0.636	0.909	0.022	2.436	0.014	2.785
S8	0.620	0.885	0.044	2.436	0.014	2.785
S9	0.603	0.862	0.066	2.435	0.014	2.785
S10	0.587	0.838	0.087	2.435	0.014	2.784
S11	0.571	0.815	0.109	2.435	0.014	2.784
S12	0.603	0.862	0.066	2.435	0.014	2.785
S13	0.587	0.838	0.087	2.435	0.014	2.784
S14	0.571	0.815	0.109	2.435	0.014	2.784
S15	0.554	0.792	0.131	2.435	0.014	2.784
S16	0.571	0.815	0.109	2.435	0.014	2.784
S17	0.554	0.792	0.131	2.435	0.014	2.784
S18	0.538	0.768	0.153	2.434	0.014	2.784

	Water	Cement	RHA	Fine Agg.	Super Plast.	Coarse Agg.
Density (kg/cum) =	1000	1440	1350	1711	1160	2152
Samples						
S19	0.538	0.768	0.153	2.434	0.014	2.784
S20	0.522	0.745	0.175	2.434	0.014	2.783
S21	0.505	0.722	0.196	2.434	0.014	2.783
S22	0.613	0.885	0.044	2.436	0.014	2.785
S23	0.603	0.87	0.058	2.435	0.014	2.785
S24	0.592	0.854	0.073	2.435	0.014	2.785
S25	0.581	0.838	0.087	2.435	0.014	2.784
S26	0.592	0.854	0.073	2.435	0.014	2.785
S27	0.581	0.838	0.087	2.435	0.014	2.784
S28	0.570	0.823	0.102	2.435	0.014	2.784
S29	0.570	0.823	0.102	2.435	0.014	2.784
S30	0.559	0.807	0.116	2.435	0.014	2.784
S31	0.549	0.792	0.131	2.435	0.014	2.784
S32	0.581	0.838	0.087	2.435	0.014	2.784
S33	0.570	0.823	0.102	2.435	0.014	2.784
S34	0.559	0.807	0.116	2.435	0.014	2.784
S35	0.559	0.807	0.116	2.435	0.014	2.784
S36	0.549	0.792	0.131	2.435	0.014	2.784
S37	0.538	0.776	0.146	2.435	0.014	2.784
S38	0.635	0.916	0.015	2.436	0.014	2.785
S39	0.624	0.901	0.029	2.436	0.014	2.785
S40	0.613	0.885	0.044	2.436	0.014	2.785
S41	0.603	0.87	0.058	2.435	0.014	2.785
S42	0.592	0.854	0.073	2.435	0.014	2.785
S43	0.624	0.901	0.029	2.436	0.014	2.785
S44	0.603	0.87	0.058	2.435	0.014	2.785
S45	0.592	0.854	0.073	2.435	0.014	2.785
S46	0.581	0.838	0.087	2.435	0.014	2.784
S47	0.570	0.823	0.102	2.435	0.014	2.784
S48	0.603	0.87	0.058	2.435	0.014	2.785
S49	0.592	0.854	0.073	2.435	0.014	2.785
S50	0.570	0.823	0.102	2.435	0.014	2.784
S51	0.559	0.807	0.116	2.435	0.014	2.784
S52	0.549	0.792	0.131	2.435	0.014	2.784
S53	0.581	0.838	0.087	2.435	0.014	2.784
S54	0.570	0.823	0.102	2.435	0.014	2.784

	Water	Cement	RHA	Fine Agg.	Super Plast.	Coarse Agg.
Density (kg/cum) =	1000	1440	1350	1711	1160	2152
Samples						
S55	0.559	0.807	0.116	2.435	0.014	2.784
S56	0.538	0.776	0.146	2.435	0.014	2.784
TOTAL	32.306	46.445	5.363	136.363	0.791	155.920

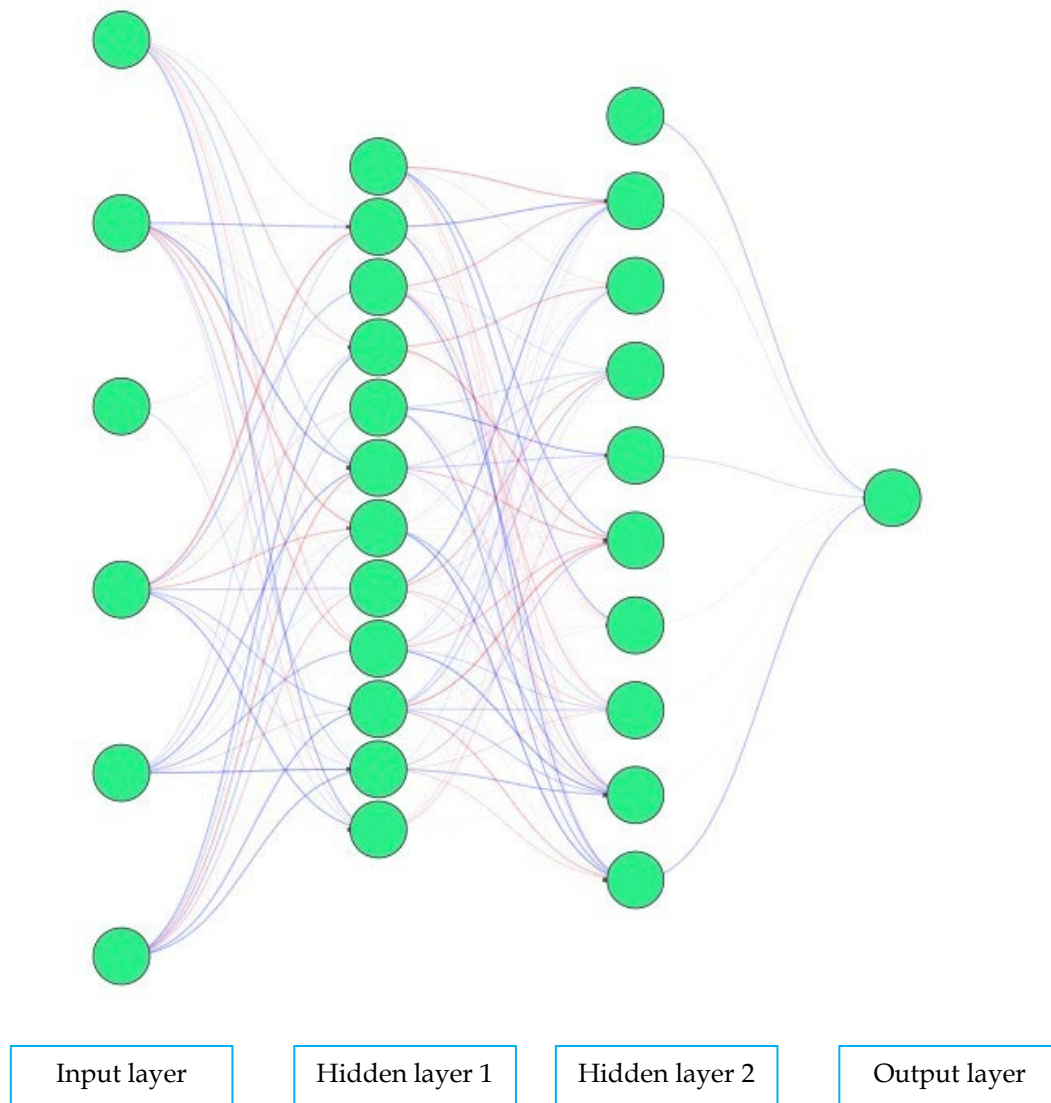


Figure 1: Artificial neural network architecture

### 3.0 Results and Discussions

#### 3.1 Oxide composition of RHAW

RHAW was burned to ash in a furnace under controlled condition at a temperature of 700°C and its chemical composition as shown in Table 4 was obtained by XRF analysis. The oxide composition indicates that the material is predominantly siliceous, with SiO<sub>2</sub> accounting for 70.606 wt.%, confirming its strong pozzolanic potential. The low contents of CaO (0.7021 wt.%) and Al<sub>2</sub>O<sub>3</sub> (0.752 wt.%) suggest that the material is non-cementitious and depends on external calcium sources to drive secondary hydration reactions. Moderate K<sub>2</sub>O (1.5957 wt.%) may require consideration due to possible alkali-silica reaction risks, although overall alkali levels remain within acceptable limits. Notably, relatively high concentrations of SrO (4.7669 wt.%) and CeO<sub>2</sub> (4.8620 wt.%) distinguish the material from conventional supplementary cementitious materials and may influence its microstructural and durability characteristics. Other oxides are present in

trace amounts and are unlikely to significantly affect bulk performance. Overall, the composition supports the classification of the material as a low-calcium, silica-rich pozzolan suitable for partial cement replacement, with expected improvements in long-term strength and durability.

Table 4: Oxide composition of RHA sample from EDXRF analysis

Oxide	Concentration (wt. %)	Oxide	Concentration (wt. %)
SiO <sub>2</sub>	70.606	Cr <sub>2</sub> O <sub>3</sub>	0.00058
P <sub>2</sub> O <sub>5</sub>	2.850	MnO	0.29521
K <sub>2</sub> O	1.5957	BaO	0.22612
MgO	2.10	La <sub>2</sub> O <sub>3</sub>	0.01625
CaO	0.7021	CeO <sub>2</sub>	4.8620
Al <sub>2</sub> O <sub>3</sub>	0.752	As <sub>2</sub> O <sub>3</sub>	[0.0004]
Fe <sub>2</sub> O <sub>3</sub>	0.3951	SeO <sub>2</sub>	1.12829
TiO <sub>2</sub>	0.05361	Br	1
ZnO	0.03734	Rb <sub>2</sub> O	0.00542
CuO	0.00234	SrO	4.7669
Ni <sub>2</sub> O	0.00185	ZrO <sub>2</sub>	0.29549
GeO <sub>2</sub>	0.00031	Nb <sub>2</sub> O <sub>5</sub>	0.51554
Ta <sub>2</sub> O <sub>5</sub>	0.01884	MoO <sub>3</sub>	1
WO <sub>3</sub>	0.0839	SnO <sub>2</sub>	1
Au	0.00300	PbO	0.00185
SO <sub>3</sub>	0.0639	Bi <sub>2</sub> O <sub>3</sub>	1
Cl	0.0221	U <sub>3</sub> O <sub>8</sub>	1
V <sub>2</sub> O <sub>5</sub>	0.00268	PdO	[0.0013]
Ag <sub>2</sub> O	0	Sb <sub>2</sub> O <sub>3</sub>	0
Co <sub>3</sub> O <sub>4</sub>	0	Cs <sub>2</sub> O	0
Ga <sub>2</sub> O <sub>3</sub>	0	Y <sub>2</sub> O <sub>3</sub>	0
PtO <sub>2</sub>	0	—	—

### 3.1 Workability of RHA - SCC

Figure 2 displays the distribution of slump values (in mm) for concrete mixes with varying percentages of Rice Husk Ash (RHA), ranging from 0% to 25% systematically. Slump value measures the workability of concrete, with higher values indicating better flow and workability. Across all RHA percentages, the slump values fluctuate between approximately 550 mm and 650 mm, showing no clear trend or significant variation as RHA content increases. The slump-flow values (550 mm –650 mm) fall within the SF1 class of self-compacting concrete as specified by [22]. For instance, at 0% RHA, slump values are spread between 550 mm and 650 mm, and this range remains consistent even at higher RHA percentages like 20%, where values are similarly distributed. The lack of a distinct pattern suggests that RHA, up to 20%, does not have a substantial impact on the workability of the concrete, as the slump values remain relatively stable across the tested range due to the efficiency of the super-plasticizer. This indicates that while RHA affects other properties like flexural strength, its influence on workability is minimal in this context.

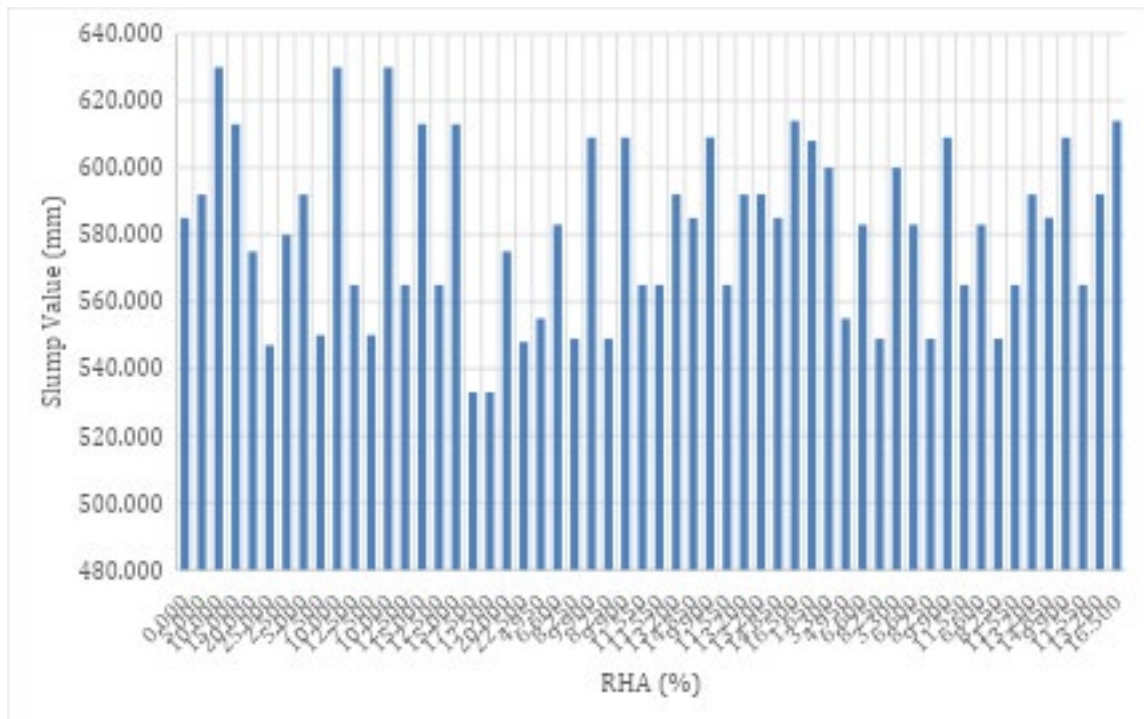


Figure 2: Relationship between RHA and slump value of SCC

### 3.2 Models and predictions

The experimental data used in this modelling consists of 56 mixture design blends, with six input features and one target output. Table 5 shows the Statistical characteristics of the dataset. Figure 3 and figure 4 illustrates the Pearson correlation coefficient between different attributes of the dataset and the pair plot. The Pearson correlation coefficient is an indicator of linear dependencies within two random variables. The correlation heat map and the pair plot both offer valuable insights into the relationships among the mix constituents and their influence on the mechanical and workability properties of the concrete samples.

Table 5: Statistical characteristic of data set

Input variables	Units	Min	Max	Mean	Standard deviation
Water	kg/m <sup>3</sup>	0.490	0.650	0.576	0.032
Cement	kg/m <sup>3</sup>	0.490	0.650	0.830	0.032
River sand	kg/m <sup>3</sup>	2.430	2.440	2.439	0.003
Granite	kg/m <sup>3</sup>	2.780	2.790	2.784	0.005
Rice husk ash (RHA)	kg/m <sup>3</sup>	0.000	0.220	0.096	0.046
Slump flow	mm	533	630	581.786	25.336
Output variables	Units	Min	Max	Mean	Standard deviation
Compressive strength	MPa	10.660	18.600	14.770	2.017
Flexural strength	MPa	2.290	3.020	2.683	0.186

Notably, there is a near-perfect positive correlation between water and cement ( $r = 0.99$ ), suggesting the use of a constant water-to-cement ratio throughout the dataset. This design choice implies a controlled approach to maintaining consistency in workability and hydration conditions across the different mixes. Conversely, rice husk ash (RHA) shows a strong negative correlation with both water and cement ( $r = -0.99$  and  $-1.00$ , respectively), indicating that RHA is used as a partial replacement for cement, with corresponding reductions in water content to preserve the water-to-binder ratio.

Further analysis reveals moderate positive correlations between compressive strength and water, cement, and fine aggregate ( $r \approx 0.5$ ), as well as a slightly stronger relationship with flexural strength ( $r = 1.00$ ), which is expected due to the similar dependency of both strength properties on the material composition. Interestingly, both compressive and flexural strengths also show a moderate positive correlation with slump value ( $r \approx 0.63$ ), implying that better workability may contribute to improved strength, possibly due to enhanced compaction and hydration. On the other hand, RHA shows a moderate negative correlation with strength properties ( $r \approx -0.48$  to  $-0.51$ ), suggesting that at the replacement levels used, RHA may reduce

strength performance, which is consistent with observations in early-age concrete incorporating pozzolanic materials that may require longer curing periods for strength development.

The pair plot reinforces these findings, with clear linear relationships observed between water and cement, compressive and flexural strength, and RHA with both cement and water. The distributions of fine and coarse aggregates are almost constant across samples, as indicated by tight vertical scatter in the pair plot and extremely low standard deviations (0.003 and 0.005, respectively). This limited variation suggests these aggregates have minimal influence on the differences observed in mechanical properties. The RHA distribution appears bimodal, suggesting the presence of two distinct groups of mixes – those with and those without RHA – which may contribute to the variability in strength and slump.

From a practical standpoint, the strong interdependence of variables like cement, water, and RHA emphasizes the importance of carefully managing substitution ratios to balance strength and workability. The positive association between slump and strength further indicates that adequate workability may enhance strength outcomes, possibly due to better compaction. Overall, the dataset suggests that concrete performance in this study is primarily driven by the binder components and their proportions, with relatively little influence from the aggregates, and that RHA replacement levels need to be optimized to mitigate the reduction in early strength while maintaining sustainability benefits.

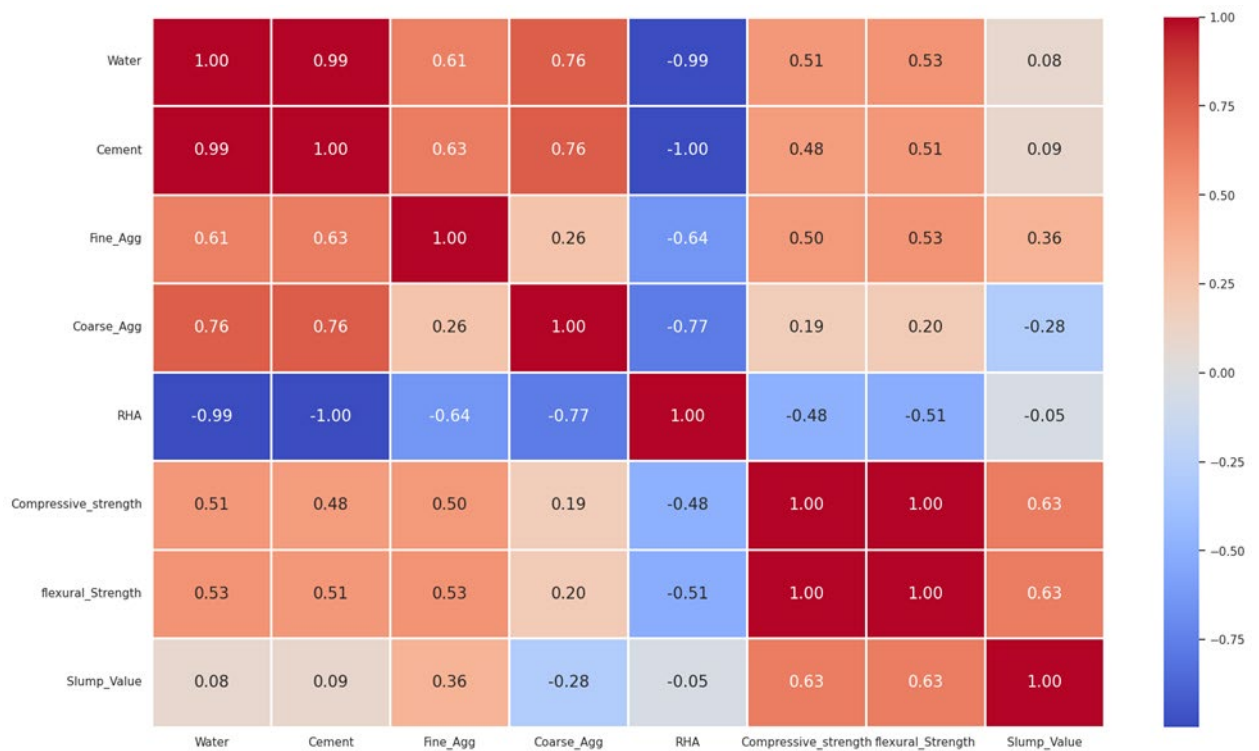


Figure 3: Pearson correlation coefficient for the dataset attribute

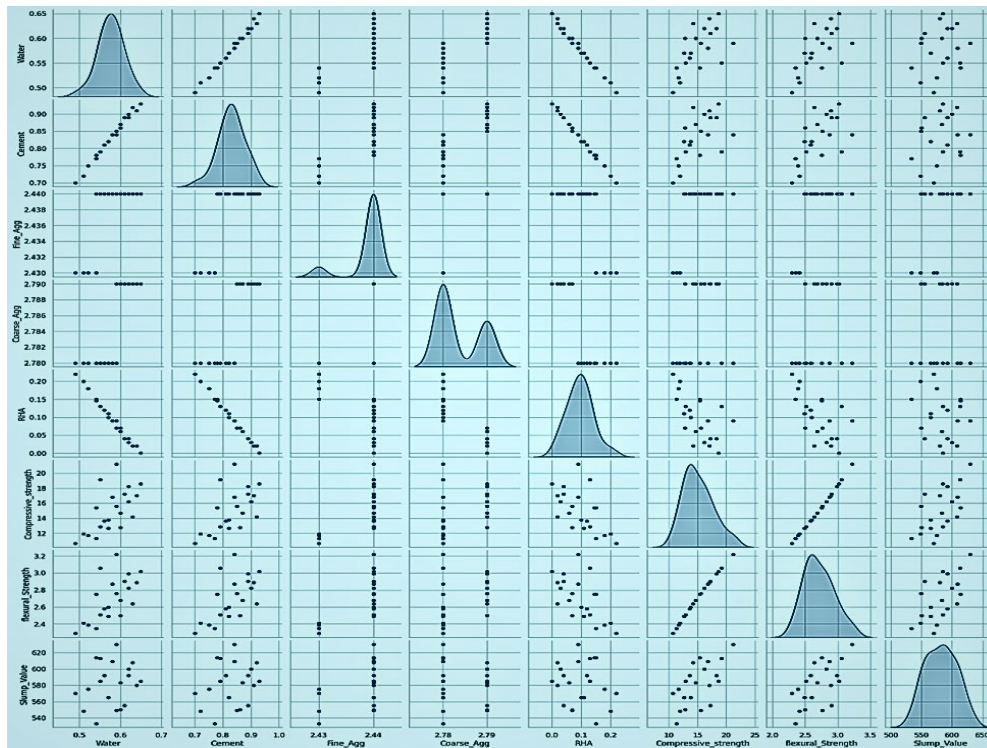


Figure 4: Pair plot for the dataset attribute

### 3.3 Linear regression prediction model

The analysis of the linear regression (LR) model outputs for Self-Compacting Concrete (SCC) reveals distinct performance levels for predicting flexural strength, Figure 5 and compressive strength Figure 6. The flexural strength plot, with an RMSE of 0.103, shows a tight clustering of data points around the  $y = x$  line, indicating a strong linear relationship and high accuracy in predictions. This low error suggests the model is reliable for estimating flexural strength, making it a valuable tool for quality control and material design where this property is critical. In contrast, the compressive strength plot, with an RMSE of 1.240, exhibits a more scattered distribution of points, indicating a less precise fit and higher prediction errors.

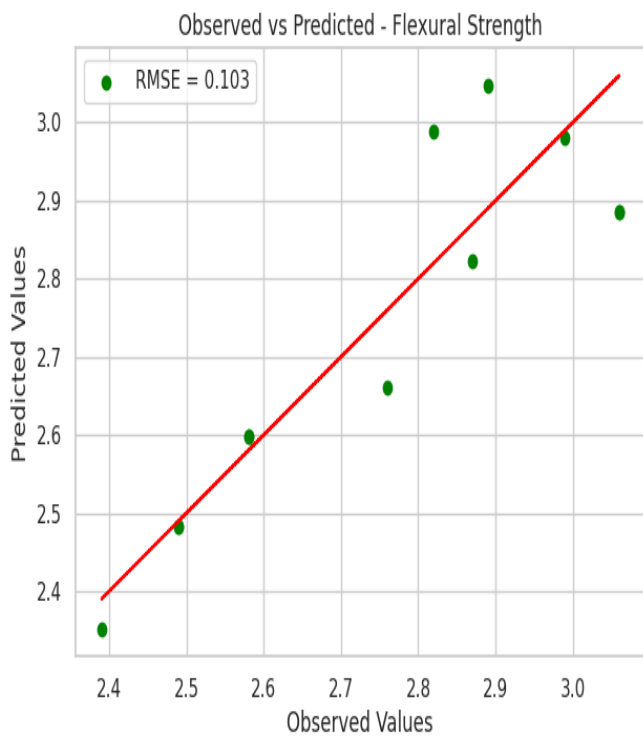


Figure 6: LR - predicted compressive strength

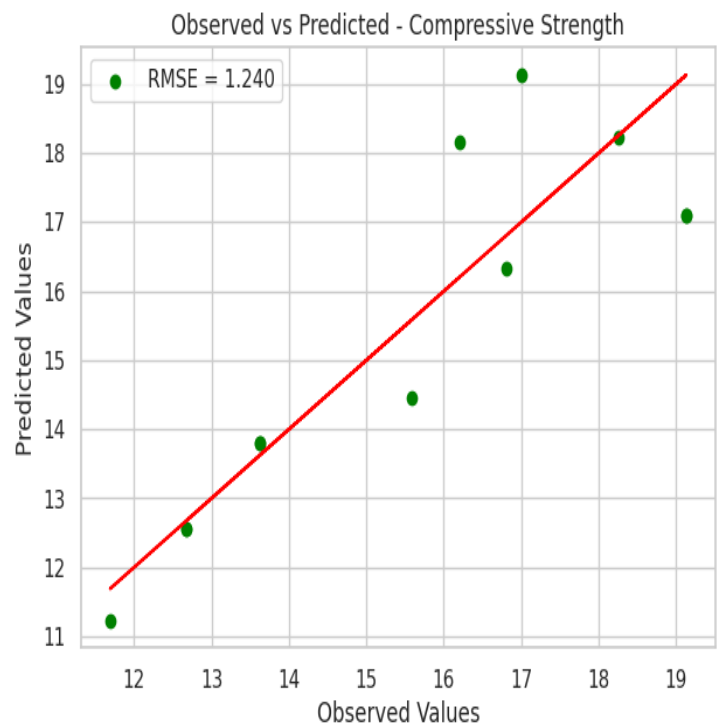


Figure 5: LR - predicted flexural strength

The larger deviation from the  $y = x$  line, particularly around mid to high values, suggests that the model struggles to capture the underlying patterns for compressive strength, possibly due to non-linear relationships or data variability. Practically, the model can be confidently applied for flexural strength predictions, but for compressive strength, further refinement is needed. Potential improvements include exploring non-linear models, incorporating additional features such as mix proportions or curing conditions, and conducting outlier analysis to address significant deviations. Cross-validation could also enhance the model's robustness, ensuring its applicability for critical engineering decisions. Overall, while the model excels in predicting flexural strength, its performance for compressive strength indicates a need for development to achieve reliable predictions.

### 3.4 Artificial neural network (ANN) prediction model

Figures 7 and 8 show the ANN prediction for the flexural and compressive strengths, respectively, of Self-Compacting Concrete (SCC). This provides the basis for a comprehensive comparison between a linear regression model and an artificial neural network (ANN) model, utilizing a dataset of 56 samples split into 80% training (approximately 45 samples) and 20% testing (approximately 11 samples). The linear regression model demonstrated superior performance for flexural strength, achieving an RMSE of 0.103 with data points tightly clustered around the  $y = x$  line, indicating high predictive accuracy and a strong linear fit. In contrast, the ANN model for flexural strength yielded a higher RMSE of 0.374, an MAE of 0.30, an MSE of 0.14, and a concerning  $R^2$  score of -0.89, suggesting it performs worse than a simple mean-based prediction and fails to capture the data's variance. For compressive strength, the linear regression model again outperformed the ANN, with an RMSE of 1.240 compared to the ANN's RMSE of 2.074 (noting a potential discrepancy with the calculated RMSE from MSE of 8.50,  $\sqrt{8.50} \approx 2.915$ ). The ANN's compressive strength metrics, MAE of 2.11, RMSE of 8.50, and a low  $R^2$  of 0.09 indicate it explains only 9% of the variance, reflecting poor predictive capability and significant scatter around the  $y = x$  line. The ANN underperformed, likely due to the small dataset size, which may not provide sufficient diversity or volume for the ANN to learn complex, non-linear relationships effectively.

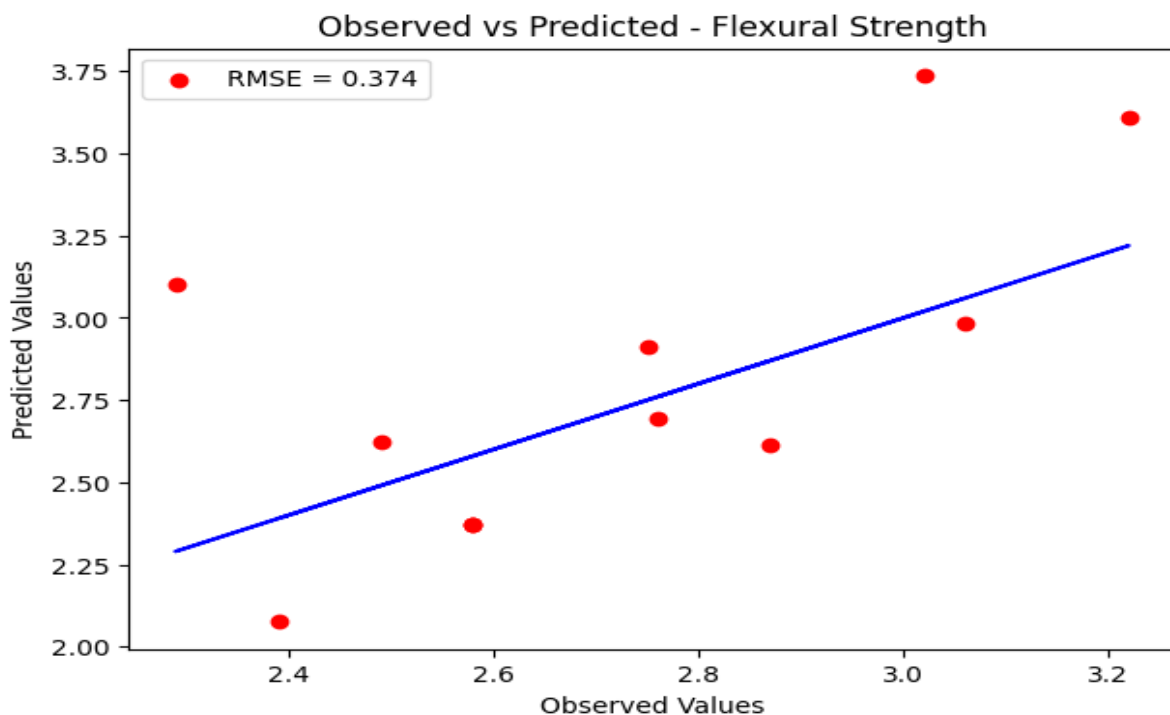


Figure 7: ANN - flexural strength

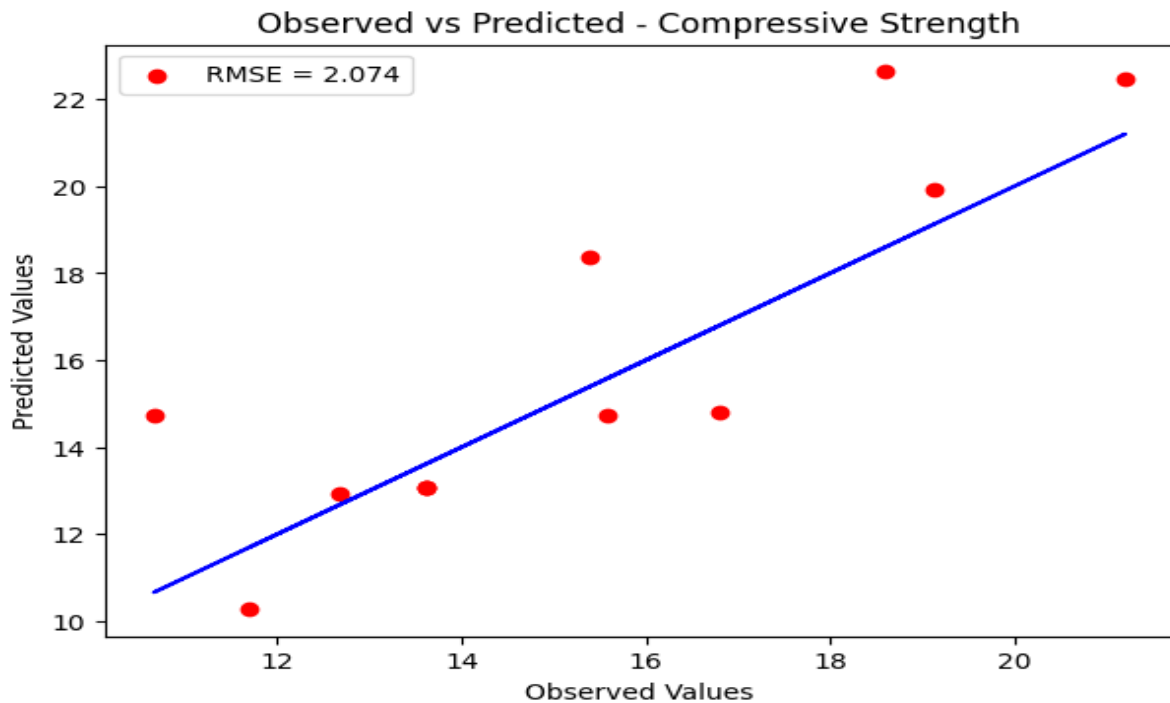


Figure 8: ANN - compressive strength

Comparatively, the linear regression model's success, particularly for flexural strength, suggests that the relationship between the input features and this property may be predominantly linear, allowing the simpler model to excel. However, for compressive strength, both models showed higher errors, with the linear regression's RMSE of 1.240 and the ANN's RMSE of 2.074 indicating that neither model fully captures the underlying patterns, possibly due to non-linearity or un-modeled factors such as mix proportions or curing conditions. The ANN's potential to model non-linear relationships was not realized, likely due to the limited dataset.

#### 4.0 Conclusion

The results presented show that it is recommended to limit RHA replacement to 5-10% in the production of SCC without compromising on its SCC properties. The linear regression model is more reliable for predicting SCC strengths, particularly flexural strength, given its lower error metrics and better fit to the data. The ANN, while theoretically capable of capturing complex patterns, underperformed due to the small dataset and likely requires a larger sample size, refined architecture (e.g., more layers or neurons), and hyperparameter optimization (e.g., adjusting the learning rate or batch size) to improve its predictive accuracy. For practical applications, the linear regression model can be confidently used for flexural strength predictions, but both models need enhancement for compressive strength, potentially through non-linear modelling approaches, additional features, or expanded datasets. Further experimentation with the ANN, including cross-validation and outlier analysis, could enhance its performance, making it a viable alternative for SCC strength prediction in future studies.

#### References

- [1] A. Alyaseen, A. Poddar, H. Alahmad, N. Kumar, and P. Sihag, "High-performance self-compacting concrete with recycled coarse aggregate: Comprehensive systematic review on mix design parameters," *J. Struct. Integr. Maint.*, vol. 8, no. 3, pp. 161-178, 2023.
- [2] J. Ahmad, Z. Zhou, and A. F. Deifalla, "Self-compacting concrete with partially substituted waste marble: A review," *Int. J. Concr. Struct. Mater.*, vol. 17, no. 25, 2023.
- [3] M. Ashar, H. A. Pratomo, and D. N. P. Sari, "The effect of superplasticizer addition on the mechanical properties of self-compacting concrete," *IOP Conf. Ser.: Mater. Sci. Eng.*, vol. 1098, no. 2, p. 022071, Feb. 2021.
- [4] Mandal, Romio, Sarat Kumar Panda, and Sanket Nayak, "Rheology of self-compacting concrete: A critical review and future perspective," *Mater. Today Proc.*, vol. 93, pp. 265-270, 2023.
- [5] Ruslan, Hanis Nadiyah, et al. "Review on performance of self-compacting concrete containing solid waste and bibliometric properties," *J. Build. Eng.*, vol. 86, p. 108752, Jun. 2024.
- [6] M. Habert et al., "Environmental impacts and decarbonization strategies in the cement and concrete industries," *Nat. Rev. Earth Environ.*, vol. 1, pp. 559-573, 2020.

- [7] Y. Zou and T. Yang, "Rice husk, rice husk ash and their applications," in *Rice Bran and Rice Bran Oil*. Urbana, IL, USA: AOCS Press, 2019, pp. 207–246.
- [8] I. Babafemi, A. John, B. Šavija, S. C. Paul, and V. Anggraini, "Engineering properties of concrete with waste recycled plastic: A review," *Sustainability*, vol. 10, no. 11, p. 3875, 2018.
- [9] M. A. Mulusew, "Prediction of compressive strength of concrete with GGBFS using neural network and fuzzy logic," *J. Mater. Civ. Eng.*, vol. 31, no. 8, p. 04019145, Aug. 2019.
- [10] W. Li, R. Wang, Q. Ai, Q. Liu, and S. X. Lu, "Estimation of compressive strength and slump of HPC concrete using neural network coupling with metaheuristic algorithms," *J. Intell. Fuzzy Syst.*, vol. 45, no. 1, pp. 577–591, 2023.
- [11] A. G. Ansari, F. A. Jokhio, M. S. S. Syed, H. Dharejo, and F. A. Memon, "Machine learning-driven approach for DDoS attacks detection using neural-based networks: A proficiency study," *Mehran Univ. Res. J. Eng. Technol.*, vol. 44, no. 3, pp. 1–13, 2025.
- [12] F. Mouawad, F. Homsy, F. Geara, and R. Mina, "Predicting compressive strength of sustainable concrete using machine learning and artificial neural networks," *Constr. Mater.*, vol. 5, no. 3, p. 56, 2025.
- [13] P. K. Mehta and P. J. M. Monteiro, *Concrete: Microstructure, Properties, and Materials*, 4th ed. New York, NY, USA: McGraw-Hill, 2014.
- [14] D. M. Khalil and S. R. Hamad, "A comparison of artificial neural network models and time series models for forecasting Turkey's monthly aluminium exports to Iraq," *J. Surv. Fish. Sci.*, vol. 10, no. 1S, pp. 4262–4279, 2023.
- [15] O. B. Olalusi and P. Spyridis, "Machine learning-based models for the concrete breakout capacity prediction of single anchors in shear," *Adv. Eng. Softw.*, vol. 147, p. 102832, 2020.
- [16] W.-K. Hong, V. T. Nguyen, and M. C. Nguyen, "Artificial intelligence-based novel design charts for doubly reinforced concrete beams," *J. Asian Archit. Build. Eng.*, vol. 21, no. 4, pp. 1497–1519, 2022.
- [17] C. Li, J. Ren, and K. Zhao, "Compressive strength prediction of rice husk ash concrete using a hybrid artificial neural network model," *Materials*, vol. 15, no. 9, p. 3135, Apr. 2022.
- [18] D. R. Eidgahee, A. Haddad, and H. Naderpour, "Assessment of shear strength parameters in granulated waste rubber using artificial neural networks and group method of data handling," *J. Cleaner Prod.*, vol. 248, p. 119223, Mar. 2020.
- [19] P. Chopra, R. K. Sharma, and M. Kumar, "Prediction of compressive strength of concrete using artificial neural network with nano-silica and rice husk ash," *Comput. Concr.*, vol. 22, no. 4, pp. 355–365, Oct. 2018.
- [20] P. G. Asteris, A. D. Skentou, P. C. Armeri, and D. J. Armaghani, "Prediction of compressive strength of self-compacting concrete using multilayer feedforward neural networks," *Appl. Soft Comput.*, vol. 97, p. 106729, Dec. 2020.
- [21] D. K. Bui, T. T. Nguyen, J. S. Chou, H. Nguyen-Xuan, and T. D. Ngo, "A hybrid artificial neural network model for predicting mechanical properties of high-performance concrete with rice husk ash," *Constr. Build. Mater.*, vol. 253, p. 119167, Aug. 2020.
- [22] EFNARC, *The European Guidelines for Self-Compacting Concrete: Specification, Production and Use*, May 2005.